

Cite this: DOI: 10.1039/c2dt31761c

www.rsc.org/dalton

PAPER

## Exceptionally high lactide polymerization activity of zirconium complexes with bridged diketiminate ligands†

Ibrahim El-Zoghbi, Todd J. J. Whitehorne and Frank Schaper\*

Received 1st August 2012, Accepted 14th September 2012

DOI: 10.1039/c2dt31761c

A cyclohexanediyl-bridged, bis(*N*-xylyl) diketiminate ligand, ( $\pm$ )-C<sub>6</sub>H<sub>10</sub>(*nacnac*<sup>Xyl</sup>H)<sub>2</sub>, LH<sub>2</sub> (Xyl = 2,6-dimethylphenyl), was obtained from the reaction of [(2,6-dimethylphenyl)amino]-pent-3-en-2-one first with Meerwein's salt, then with ( $\pm$ )-cyclohexanediamine. The reaction of the ligand with Zr(NMe<sub>2</sub>)<sub>4</sub> yielded LZr(NMe<sub>2</sub>)<sub>2</sub>. Protonation of the remaining diamide ligands with EtOH or [H<sub>2</sub>NMe<sub>2</sub>]Cl yielded LZr(OEt)<sub>2</sub> and LZrCl<sub>2</sub>, respectively. The latter complex was also obtained by the reaction of LH<sub>2</sub> first with *n*BuLi and then with ZrCl<sub>4</sub>(THF)<sub>2</sub>. The dichloride complex yielded LZr(OEt)<sub>2</sub> and LZrMe<sub>2</sub> upon reaction with NaOEt or MeLi/AlMe<sub>3</sub>, respectively. X-ray diffraction studies showed a *trans*-configuration of the ancillary ligands in LZrCl<sub>2</sub> and LZrMe<sub>2</sub>, and a *cis*-configuration in LZr(NMe<sub>2</sub>)<sub>2</sub> and LZr(OEt)<sub>2</sub>. LZr(OEt)<sub>2</sub> was tested as a catalyst for the polymerization of *rac*-lactide. Kinetic investigations yielded a rate law first order in catalyst and monomer and a rate constant  $k = 14(1) \text{ L mol}^{-1} \text{ s}^{-1}$ , the latter being orders of magnitude higher than typical activities for group 4 complexes in lactide polymerization. Analyses of the obtained polymer revealed an atactic polymer and broad polymer molecular weight distributions with sizeable fractions of cyclic oligomers. The influence of contaminants on the polymerization activity was examined: while lactic acid deactivates the catalyst, addition of up to 1 equiv. of water or *para*-toluenesulfonic acid revitalized catalysts not showing maximum activity.

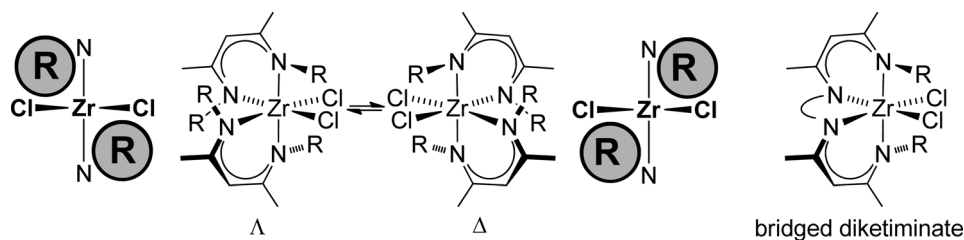
## Introduction

The increased popularity of  $\beta$ -diketiminate (“*nacnac*”) ligands led to several investigations of their coordination chemistry with zirconium in the last two decades. The obtained complexes can be summarized in three types: *nacnac*ZrX<sub>3</sub>L<sub>0–1</sub>,<sup>1–10</sup> pseudo-tetrahedral Cp<sup>R</sup>(*nacnac*)ZrX<sub>2</sub>,<sup>3,5,10–19</sup> and octahedral *nacnac*<sub>2</sub>ZrX<sub>2</sub>.<sup>3–5,20–23</sup> The coordination mode of the diketiminate ligand in all of these complexes can vary between simple *N,N'*- $\kappa^2$ -coordination and higher coordination modes such as “ $\eta^5$ -like” or a  $\kappa^2, \eta^2$ -coordination.<sup>19,24</sup> Octahedral zirconium bisdiketiminate complexes, *nacnac*<sub>2</sub>ZrX<sub>2</sub>, or their respective cations, [*nacnac*<sub>2</sub>ZrX]<sup>+</sup>, are very attractive targets as catalysts for coordination–insertion polymerization or related reactions: (i) They show the least variation in diketiminate binding modes (in nearly all complexes a simple  $\kappa^2$ -coordination is observed). (ii) They contain two reactive sites, which are forced in a *cis*-position with each other, since the *N*-substituents disfavour an assembly of all nitrogen atoms in the same plane.<sup>23</sup> (iii) The fixed C<sub>2</sub>-symmetry

of the chiral metal complex renders the coordination sites homotopic and allows stereoselectivity of the catalysed reaction. (iv) Last but not least, the *N*-substituents in an idealized *cis*-octahedral structure are ideally placed to exert control on the reaction (Scheme 1). Unfortunately, *ortho*-substituted *N*-aryl diketimines are sterically too demanding to form bisdiketiminate complexes and *nacnac*<sup>Ar</sup><sub>2</sub>ZrX<sub>2</sub> complexes were limited to ligands where at least one *N*-substituent lacks *ortho*-substituents.<sup>3–5,21</sup> We recently reported that diketimines with *N*-alkyl substituents form the desired C<sub>2</sub>-symmetric bisdiketiminate complexes, *nacnac*<sup>R</sup><sub>2</sub>ZrX<sub>2</sub>, even with sterically demanding *N*-alkyl substituents such as cyclohexyl or  $\alpha$ -methylbenzyl.<sup>23</sup> Application of these compounds in catalytic reactions has been, however, prevented by the high steric crowding, which shielded the active sites from further reactions. Thus, *nacnac*<sup>R</sup><sub>2</sub>ZrCl<sub>2</sub> (R = benzyl, cyclohexyl,  $\alpha$ -methylbenzyl) failed to react either with a variety of alkylating reagents such as MeLi, *n*BuLi, AlMe<sub>3</sub>, MeMgX, or ZnEt<sub>2</sub>, or with sodium ethoxide. The corresponding dimethyl complex *nacnac*<sup>Bn</sup><sub>2</sub>ZrMe<sub>2</sub> reacted with B(C<sub>6</sub>F<sub>5</sub>)<sub>3</sub>, but the obtained cationic zirconium methyl complex reacted neither with diphenylacetylene nor benzaldehyde, most likely due to steric blocking of the metal center.<sup>23</sup> In addition to the low reactivity at the “active coordination sites”, the configuration of the complexes was not stable. As observed for *N*-aryl complexes,<sup>3–5</sup> Bailar-Twist isomerisation led to fast interconversion between  $\Delta$ - and  $\Lambda$ -enantiomers at room temperature on the NMR time scale (Scheme 1), which could not be prevented even by the use of a chiral

Département de chimie, Université de Montréal, Montréal, Québec H3C 3J7, Canada. E-mail: Frank.Schaper@umontreal.ca

† Electronic supplementary information (ESI) available: Tables S1–S6, investigations regarding variations in catalyst activity, variable temperature NMR data, details of polymerization experiments, Crystallographic Information Files (CIF). CCDC 894423–894426. For ESI and crystallographic data in CIF or other electronic format see DOI: 10.1039/c2dt31761c



Scheme 1

*N*-substituent.<sup>23</sup> To address both problems, we decided to connect the two diketiminate ligands by a cyclohexanediyl bridge (Scheme 1). The smaller bite angle enforced by the C<sub>2</sub>-bridge should provide easier access to the reactive sites, while its axial chirality should prevent the Δ–Λ-isomerisation. Similar bisdiketiminate ligands with achiral (CH<sub>2</sub>)<sub>*n*</sub>-bridges (*n* = 2, 3) were previously employed by Gong *et al.*, but the respective zirconium complexes still showed fast Δ–Λ-isomerisation in solution.<sup>22</sup> Herein we report the preparation and structural analysis of C<sub>6</sub>H<sub>10</sub>(*nacnac*<sup>Xyl</sup>)<sub>2</sub>ZrX<sub>2</sub> complexes (Xyl = 2,6-dimethylphenyl), their reactivity compared to unbridged analogues and in *rac*-lactide polymerization.

## Results and discussion

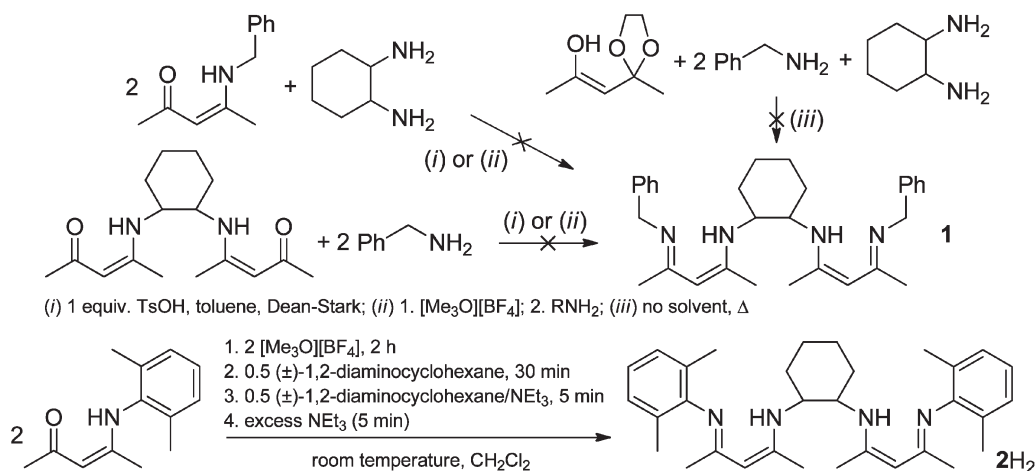
### Ligand synthesis

As a close analogue to the *N*-alkyl bisdiketiminate complexes studied before,<sup>23</sup> we attempted to prepare the bridged ligand **1** with *N*-benzyl substituents (Scheme 2). However, independent of the starting point of the reaction or the synthetic path used (acid-catalysed water elimination, alkylation with Meerwein's salt, use of ethyleneketal), either no reaction occurred or inseparable product mixtures were obtained. This was in agreement with previous observations in our group: while several non-symmetrically substituted *N*-aryl diketimines have been reported, we were unable to isolate a mixed *N*-alkyl diketimine. Closer investigations indicated that attack at the imine group was faster than the attack at the keto group, leading to scrambling of the

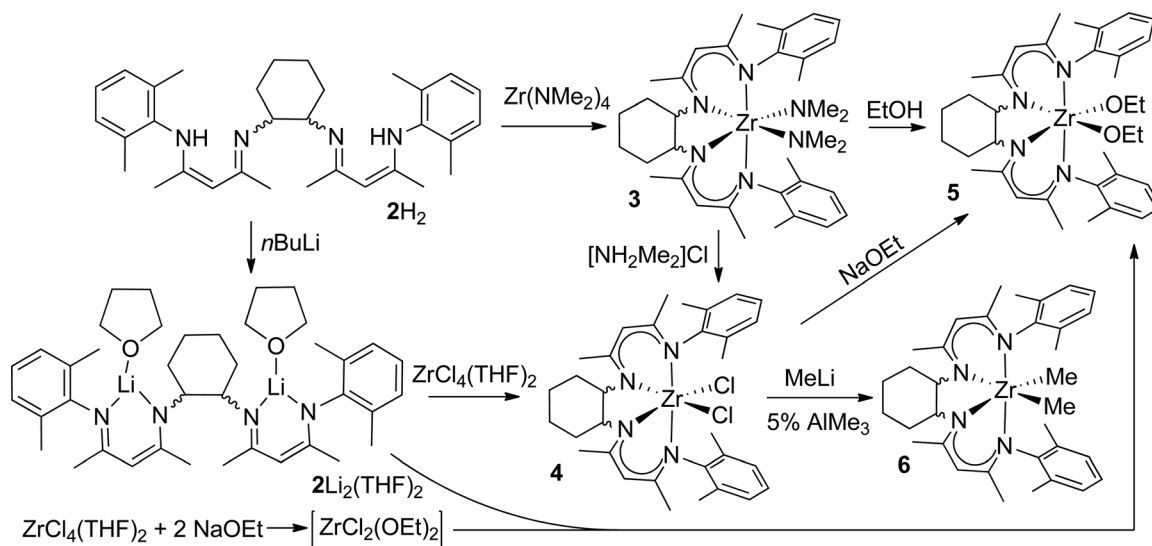
*N*-substituents and – in the best cases – to statistical product mixtures.<sup>25</sup> However, due to the favoured formation of *N*-aryl imines over *N*-alkyl imines, a more than statistical yield of a mixed diketimine was obtained, when acetylacetone was reacted with mixtures of aniline and amine.<sup>25</sup> We thus decided to employ *N*-xylyl substituents and obtained the bridged ligand C<sub>6</sub>H<sub>10</sub>(*nacnac*<sup>Xyl</sup>)<sub>2</sub>H<sub>2</sub>, **2H<sub>2</sub>**, in 76% yield (Scheme 2). Reaction conditions were chosen to disfavour *N*-substituent scrambling. Thus, acetylacetone was first reacted with aniline to form the respective enamine. Instead of the acid-catalysed condensation we normally employ for symmetric *N*-alkyl diketimines and which requires long reaction times,<sup>25</sup> we followed a synthetic protocol used for closely related ligands<sup>26–28</sup> and used Meerwein's salt to activate the enamine ([Me<sub>3</sub>O][BF<sub>4</sub>] worked slightly better than the respective ethyl salt in our hands). Nevertheless, the reaction outcome was very sensitive to the reaction times involving amines. Either addition of NEt<sub>3</sub> directly with the amine or prolonged reaction times (steps 2–4, Scheme 2) drastically reduced isolated yields of **2H<sub>2</sub>**.

### Complex syntheses

Reactions of ligand **2H<sub>2</sub>** with ZrBn<sub>4</sub> under various conditions did not yield an isolable product. Zr(NMe<sub>2</sub>)<sub>4</sub> proved to be more reactive and yielded 50% conversion in solution (C<sub>6</sub>D<sub>6</sub>, 60 °C). Reaction in the absence of a solvent at 120 °C then afforded the diamido complex **3** (Scheme 3) in 71% crystallized yield. The latter complex reacted with dimethylammonium chloride or ethanol to yield the respective dichloride and diethoxide



Scheme 2



Scheme 3

complexes **4** and **5** (Scheme 3). The protonation reaction, however, was unselective and in both cases protonation of the bisdiketiminate ligand occurred in significant amounts (up to 50%). Complex **4** was obtained, however, in good yields following a salt metathesis route: deprotonation of bisdiketiminate ligand **2H<sub>2</sub>** with *n*BuLi in THF yielded the ligand dilithium salt **2Li<sub>2</sub>(THF)<sub>2</sub>** (Scheme 3). Spectroscopic data and combustion analysis suggest the coordination of one THF molecule per lithium atom, as usually observed for diketiminate lithium salts containing coordinated THF or diethyl ether. A further reaction between **2Li<sub>2</sub>(THF)<sub>2</sub>** and ZrCl<sub>4</sub>(THF)<sub>2</sub> yielded the zirconium dichloride complex **4** in 80% yield (Scheme 3). Contrary to the unbridged bis(diketiminate) zirconium complexes, *nacnac*<sup>R</sup><sub>2</sub>ZrCl<sub>2</sub>, which did not react with MeLi even at higher temperatures,<sup>23</sup> reaction of dichloride complex **4** with MeLi at room temperature in C<sub>6</sub>D<sub>6</sub> afforded complete conversion of the dichloride to the respective dimethyl complex **6** (contaminated with significant amounts (35%) of the monomethylation product) in less than 5 min (Scheme 3). Constraining the ligand by introduction of a cyclohexanediyl bridge thus indeed resulted in the intended increase of reactivity. Analytically pure dimethyl complex **6** was isolated from large-scale reactions employing MeLi and a catalytic amount of AlMe<sub>3</sub> in 36% yield. Dichloride **4** also proved to be more reactive than unbridged bisdiketiminate complexes towards NaOEt<sup>23</sup> and cleanly yielded the diethoxy complex **5** (Scheme 3), albeit under harsher reaction conditions (3 d, 110 °C). Complex **5** can be prepared directly from ZrCl<sub>4</sub>(THF)<sub>2</sub> under milder conditions (12 h, 80 °C) and with identical yields, if ZrCl<sub>4</sub>(THF)<sub>2</sub> is first reacted with NaOEt<sub>2</sub> and then with **2Li<sub>2</sub>(THF)<sub>2</sub>**. Formation of a putative ZrCl<sub>2</sub>(OEt)<sub>2</sub> intermediate is crucial. The direct reaction of ZrCl<sub>4</sub> with a mixture of NaOEt and **2Li<sub>2</sub>(THF)<sub>2</sub>** still yielded **5**, but again required 3 d of reaction time.

**Solid state and solution structures.** The solid state structures of complexes **3–6** are shown in Fig. 1–4. Compared to unbridged bisdiketiminate zirconium complexes, the constraint introduced by bridging the diketiminate ligands results in a severe distortion

of the octahedral geometry. The bridgehead nitrogen atoms (N1 and N3) are severely tilted out of the ZrX<sub>2</sub> plane (38–49° in *cis*-C<sub>2</sub>-bridged, 8 ± 5° in unbridged complexes, Table 1). The reduced bite-angle enforced by the bridge (N1–Zr–N3 = 70–73° in C<sub>2</sub>-bridged, 89 ± 3° in unbridged complexes) further results in a widening of the ZrX<sub>2</sub> angles of the atoms *trans* to the bridgehead nitrogen atoms (117–138° in *cis*-C<sub>2</sub>-bridged, 91 ± 3° in unbridged complexes) and slightly elongated (≈0.01 Å) Zr–N distances for the non-bridgehead nitrogen atoms. A structural effect of bridging favourable for potential applications is a slight change in the position of the xylyl substituents. While the *N*-substituents in unbridged diketiminate complexes were positioned between the ZrCl<sub>2</sub>-fragment (C–N–Zr–Cl torsion angles > 27°, Table 1), they are eclipsed with one Zr–X bond in bridged complexes (C–N–Zr–X torsion angles < 14°).

Of the possible structural isomers of C<sub>6</sub>H<sub>10</sub>(*nacnac*<sup>Xyl</sup>)<sub>2</sub>ZrX<sub>2</sub> complexes, only C<sub>2</sub>-symmetric isomers **A** and **C** were observed in the solid state (Scheme 4). Complexes **3** and **5** show a *cis*-X<sub>2</sub> configuration<sup>22</sup> in the solid state, as was observed for all other bisdiketiminate zirconium complexes reported (X–Zr–X angle = 89–117°).<sup>3,4,20–23</sup> In both cases, the *S,S,Δ/R,R,Λ*-isomer (**A**, Scheme 4) was observed, while the *S,S,Λ/R,R,Δ*-isomer (**B**, Scheme 4) was absent. Complexes **4** and **6** crystallize as the *trans*-isomer (**C**, Scheme 4). While variable temperature NMR investigations have shown that for unbridged diketiminate complexes a *trans*-Cl configuration is not obtained even as a short-lived intermediate at elevated temperatures,<sup>23</sup> the decreased N1–Zr–N3 angle in **4** and **6**, caused by the cyclohexanediyl bridge, enables the placement of all four nitrogen atoms in the equatorial plane. The preference for the *trans*-arrangement of the chloride atoms in **4** is nevertheless surprising, since structures of *cis*-**3** and *cis*-**5** are nearly superposable with *cis*-C<sub>2</sub>H<sub>4</sub>(*nacnac*<sup>dipp</sup>)<sub>2</sub>ZrCl<sub>2</sub> (dipp = 2,6-diisopropylphenyl, see also Fig. 5b),<sup>22</sup> indicating that neither the cyclohexanediyl bridge nor the chloride ligands should prevent formation of a *cis*-Cl complex. Most likely, the *trans*-configuration is sterically slightly more favourable, but only for small ligands, such as chloride or methyl. Space-filling diagrams of **4** and **6** indicate that increased steric

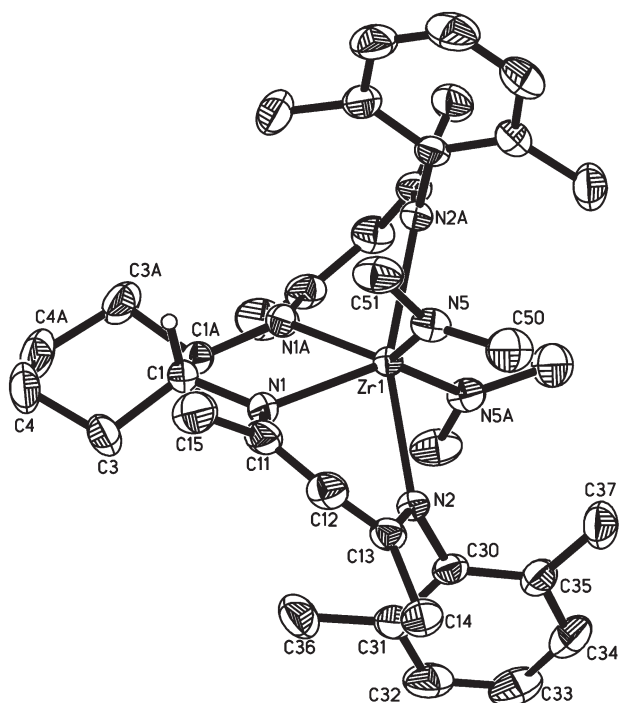


**Fig. 1** X-ray structure of **3**. Thermal ellipsoids are drawn at the 50% probability level. Most hydrogen atoms were omitted for clarity.

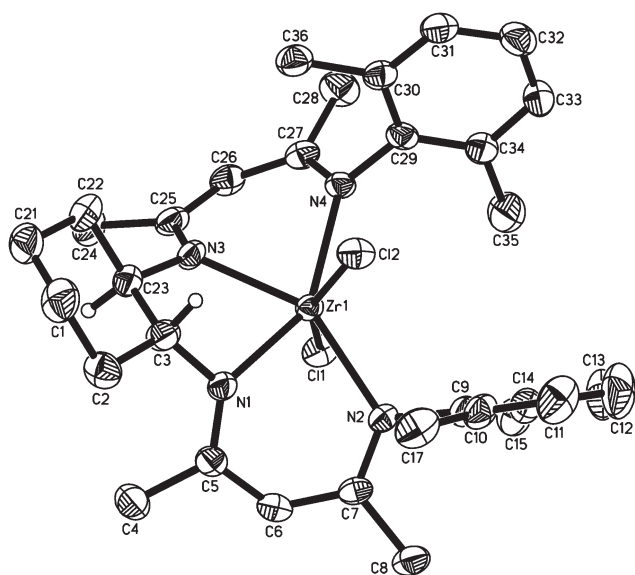


**Fig. 2** X-ray structure of **4**. Thermal ellipsoids are drawn at the 50% probability level. Most hydrogen atoms and co-crystallized benzene were omitted for clarity.

demand, either of the ancillary ligand (as in **3** or **5**) or of the *ortho*-substituents on the phenyl ring (as in  $C_2H_4(nacnac^{dipp})_2-ZrCl_2$ ), would destabilize the *trans*-configuration. Additionally,  $\pi$ -donation from the OEt or the  $NMe_2$  substituents in **3** and **5** might further favor a *cis*-geometry for these complexes.

The preference of *cis*-complexes **3** and **5** to form the *S,S,S*/ $\Delta$ /*R,R,\Lambda*-isomer (**A**, Scheme 4) seems intuitively correct on a first

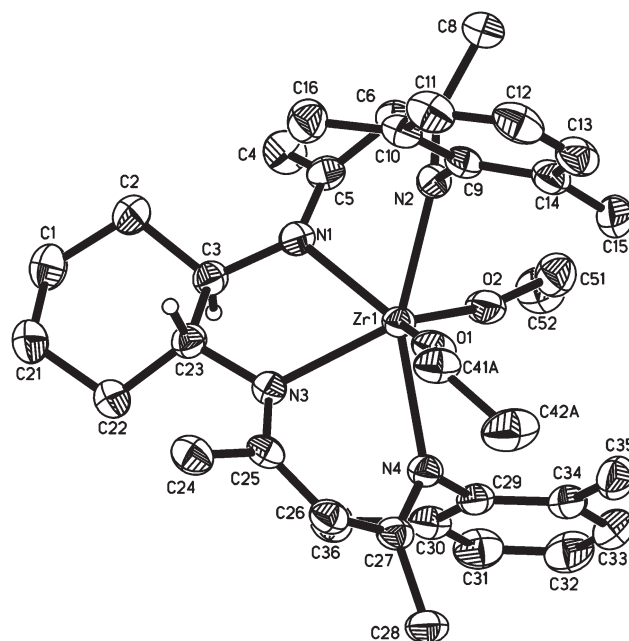


**Fig. 3** X-ray structure of **5**. Thermal ellipsoids are drawn at the 50% probability level. Most hydrogen atoms and the disorder of one OEt group were omitted for clarity.

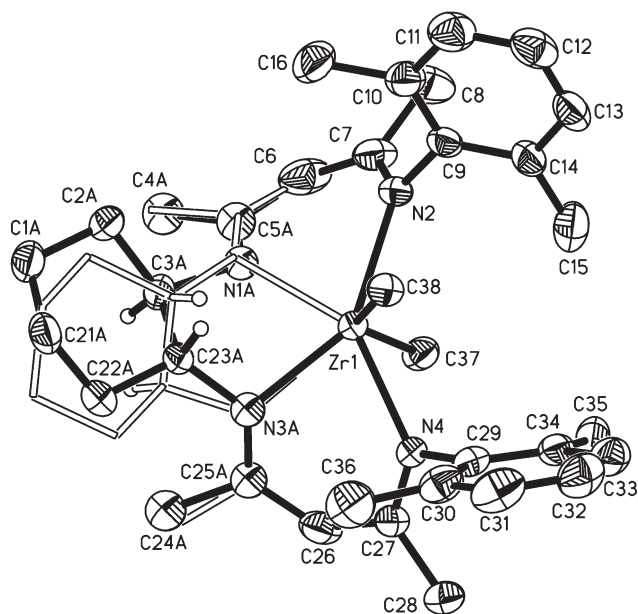


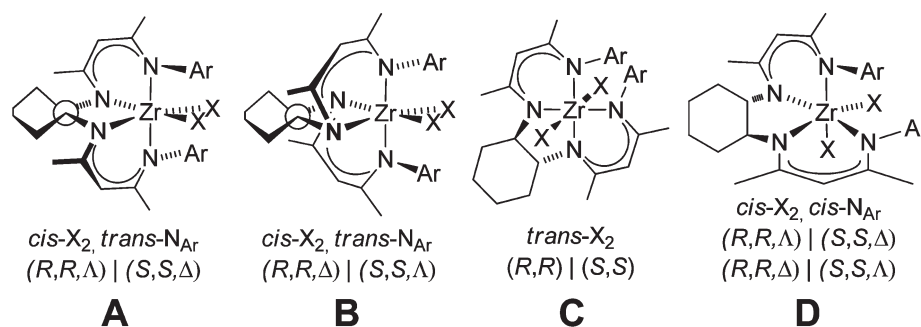
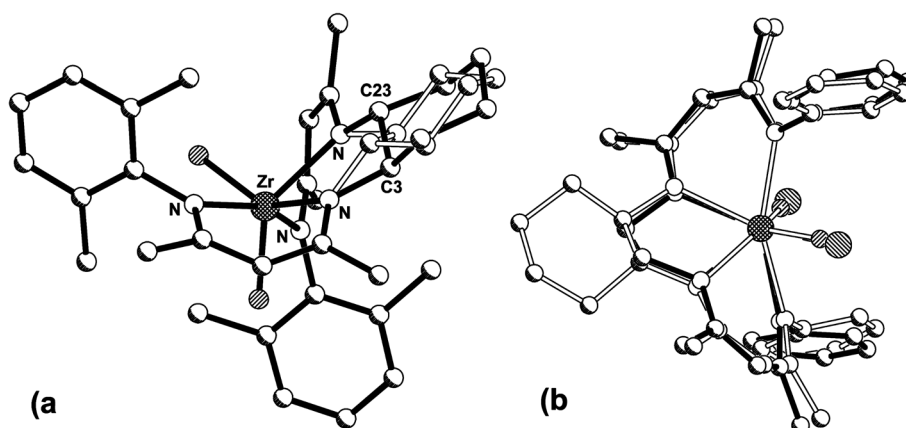
**Fig. 4** X-ray structure of **6**. Thermal ellipsoids are drawn at the 50% probability level. Most hydrogen atoms were omitted for clarity. The smaller fraction of the disordered cyclohexanediamine bridge is shown in open lines without thermal ellipsoids or labelling.

glance. Since the diketimate bite-angle of  $74-78^\circ$  (Table 1) is significantly smaller than the ideal octahedral angle, nitrogen atoms N1 and N3 *trans* to the ancillary ligands are slightly displaced out of the  $ZrX_2$  plane (Fig. 1 and 3). In the case of the  $\Lambda$ -isomer, an *R,R*-cyclohexanediamine bridge seems to accommodate this deformation more readily than the *S,S*-configuration

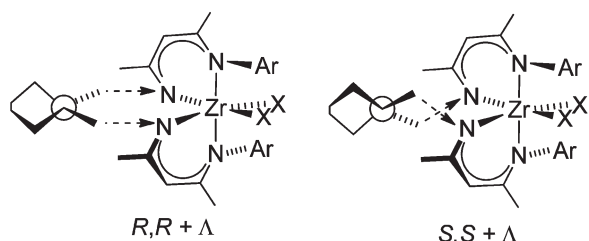
**Table 1** Bond distances [ $\text{\AA}$ ] and bond angles [ $^\circ$ ] in the crystal structures of 3–6

	3	4	5	6	<i>nacnac</i> <sup>R</sup> <sub>2</sub> ZrCl <sub>2</sub> <sup>a</sup>	C <sub>2</sub> H <sub>4</sub> ( <i>nacnac</i> <sup>dipp</sup> ) <sub>2</sub> ZrCl <sub>2</sub> <sup>b</sup>
Zr–N1/N3	2.252(1)	2.183(2), 2.211(2)	2.256(2), 2.226(2)	2.190(5)–2.250(7)	2.23 ± 0.05	2.175(3)
Zr–N2/N4	2.374(1)	2.285(2), 2.277(2)	2.307(2), 2.344(2)	2.315(3), 2.344(3)	2.22 ± 0.05	2.318(4)
Zr–X <sup>c</sup>	2.068(1)	2.425(1), 2.438(1)	1.937(2), 1.941(2)	2.265(4), 2.283(3)	2.45 ± 0.06	2.422(2)
N1–Zr–N3 <sup>d</sup>	71.92(7)	72.26(8)	72.32(7)	70.1(2), 72.0(2)	89 ± 3	72.68(11)
N2–Zr–N4 <sup>d</sup>	159.47(7)	133.18(8)	156.14(7)	138.4(1)	165 ± 13	160.03(10)
N1–Zr–N2	74.36(5)	77.97(8)	76.41(7)	75.5(1), 75.9(2)		
N3–Zr–N4		77.85(8)	74.82(7)	75.0(1), 76.2(2)		
X–Zr–X <sup>c</sup>	124.93(8)	156.24(3)	121.13(8)	138.0(1)	91 ± 3	117.40(4)
(Zr/N1/N3)–(Zr/X1/X2) <sup>c,d</sup>	49	80	49	80, 81	8 ± 5	38
(Zr/N1/N3)–(Zr/N2/N4) <sup>c</sup>	44	12	44	9, 10	83 ± 7	53
C–N2/4–Zr–X <sup>e</sup>	13	—	1, 10	—	37 ± 10	3, 6

<sup>a</sup> Taken from ref. 23. <sup>b</sup> Taken from ref. 22. <sup>c</sup> 4: X = Cl1, Cl2; 3: X = N5, N5A; 5: X = O1, O2; 6: X = C37, C38. <sup>d</sup> For 3: N3 = N1A, N4 = N2A. For 6: N1 = N1A/B, N3 = N3A/B. <sup>e</sup> Torsion angle between the N-substituent and the ancillary ligand on Zr.

**Scheme 4**

**Fig. 5** (a) X-ray structure of (*R,R,Λ*)-5 with an idealized *S,S*-cyclohexanediamine fitted into the structure (hollow lines). (b) Best fit overlay of C<sub>2</sub>H<sub>4</sub>(*nacnac*<sup>dipp</sup>)<sub>2</sub>ZrCl<sub>2</sub><sup>22</sup> and 5. Ethyl groups, aryl substituents and hydrogen atoms were omitted for clarity.

**Scheme 5**

(Scheme 5). To investigate in more detail this simplistic explanation, which neglects the strong deviation from octahedral geometry observed in 3 and 5, as well as the typical distortion of the diketiminato ligand into a boat-like conformation,<sup>19,24</sup> an idealized *S,S*-cyclohexanediamine bridge was fitted into the crystal structure of  $\Lambda$ -5 (Fig. 5a). The change of the configuration in the cyclohexanediamine bridge requires a higher bending of the N–C3/C23 bond out of the diketiminato mean plane ( $52^\circ$  for the hypothetical *S,S,Λ*-isomer depicted in Fig. 5a,  $24 \pm 3^\circ$  for the

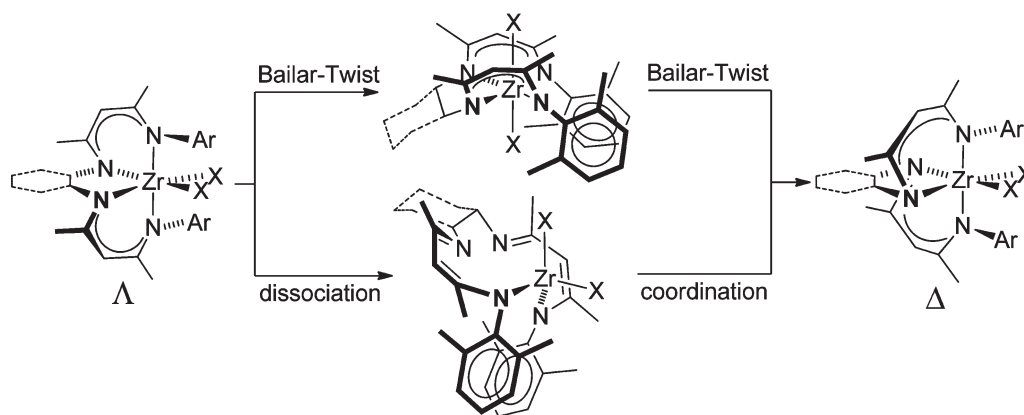
*R,R*, $\Lambda$ -isomers **3** and **5**). This latter value is very close to the out-of-plane bending of the *N*-substituent in unbridged *N*-alkyl bisdiketiminato complexes (16–24°)<sup>23</sup> and in C<sub>2</sub>H<sub>4</sub>- and C<sub>3</sub>H<sub>6</sub>-bridged bisdiketiminato complexes (24–33°).<sup>22</sup> In fact, crystal structures of **5** and the C<sub>2</sub>H<sub>4</sub>-bridged complex C<sub>2</sub>H<sub>4</sub>(*nacnac*<sup>dipp</sup>)<sub>2</sub>ZrCl<sub>2</sub><sup>22</sup> are nearly superposable (Fig. 5b), indicating the correct stereochemical match between an *R,R*-configured cyclohexanediyl bridge and a  $\Lambda$ -configuration at the metal center.

In solution, proton NMR spectra of **3–6** show one signal for the methine protons of the cyclohexane ring, one signal for the central CH resonance of the diketiminato ligand, two signals for the diketiminato methyl groups and two signals for the xylyl methyl groups. The C<sub>2</sub>-symmetry of the ligand is thus preserved in the complex (either by symmetry or fast isomerisation). The presence of two xylyl methyl resonances, of three aromatic resonances in proton NMR spectra of **3–6**, as well as of four resonances for the aromatic ring in carbon NMR spectra of **3–6**, and the fact that two xylyl methyl resonances were observed also for lithium complex 2Li<sub>2</sub>(THF)<sub>2</sub> and the free ligand 2H<sub>2</sub> (see the Exp. section), all indicate that *N*-aryl rotation is slow on the NMR time scale. In agreement with hindered *N*-aryl rotation, NMR spectra of **5** did not indicate any coalescence of the xylyl methyl groups up to 70 °C.

Unbridged diketiminato complexes have shown evidence for fast  $\Delta$ - $\Lambda$ -isomerisation in solution (**A**  $\leftrightarrow$  **B**, Scheme 4) by a Bailar-Twist mechanism.<sup>3–5,23</sup> Despite the introduction of a bridging group, the same fast isomerisation was observed by Dong *et al.* in C<sub>2</sub>H<sub>4</sub>- or C<sub>3</sub>H<sub>6</sub>-bridged complexes: coalescence of the CH<sub>2</sub> protons in the bridge yielded averaged C<sub>2v</sub>-symmetric NMR spectra,<sup>22</sup> in the case of a C<sub>2</sub>H<sub>4</sub>-bridge even at –70 °C. NMR spectra of **3–6** do not contain any group which would coalesce in the case of a fast  $\Delta$ - $\Lambda$ -isomerisation and thus no straightforward way to establish the absence or presence of  $\Delta$ - $\Lambda$ -isomerisation. However, while spectra of C<sub>2</sub>H<sub>4</sub>(*nacnac*<sup>Xyl</sup>)<sub>2</sub>ZrCl<sub>2</sub> displayed only one resonance for the xylyl methyl group even at low temperatures,<sup>22</sup> two xylyl methyl resonances were observed in spectra of **3–6**. In the absence of *N*-xylyl rotation (*vide supra*), the equivalence of the xylyl methyl groups in C<sub>2</sub>H<sub>4</sub>(*nacnac*<sup>Xyl</sup>)<sub>2</sub>ZrCl<sub>2</sub> has to be caused by passage through a C<sub>2v</sub>-symmetric intermediate associated with the  $\Delta$ - $\Lambda$ -isomerisation. Direct  $\Delta$ - $\Lambda$ -isomerisation of bridged bisdiketiminato

complexes by a Bailar-Twist would result in an isomer with the bridgehead nitrogen atoms in an impossible *trans*-configuration. Contrary to unbridged *nacnac*<sup>R</sup>-ZrX<sub>2</sub> complexes,  $\Delta$ - $\Lambda$ -isomerisation *via* a Bailar-Twist mechanism thus has to pass by a *trans*-X<sub>2</sub> complex (Scheme 6). Alternatively, based on the fact that isomerisation is faster for C<sub>2</sub>H<sub>4</sub>- than for C<sub>3</sub>H<sub>6</sub>-bridged complexes, Dong *et al.* had proposed that  $\Delta$ - $\Lambda$ -isomerisation in bridged bisdiketiminato complexes proceeds by dissociation of the bridging nitrogen atoms and through a tetrahedral intermediate rather than *via* a Bailar-Twist mechanism (Scheme 6).<sup>22</sup> Although only two structurally characterized examples of  $\kappa^1$ -coordinated diketiminato ligands were reported,<sup>29,30</sup> such an intermediate does not seem unreasonable, in particular considering the steric strain introduced by the bridge. In the case of C<sub>2</sub>H<sub>4</sub>-bridged complexes, the *trans*-X<sub>2</sub> complex as well as the four-coordinated intermediate easily achieve apparent C<sub>2v</sub>-symmetry by a ring inversion of the metallacycle(s) and  $\Delta$ - $\Lambda$ -isomerisation would thus lead to the observed equalization of the xylyl methyl groups for C<sub>2</sub>H<sub>4</sub>-bridged complexes (Scheme 6). In **3–6**, even fast inversion of the metallacycle(s) of the same intermediates results only in apparent C<sub>2</sub>-symmetry and the inequivalence of the xylyl methyl groups is preserved. (In fact, if **4** and **6** retain the C<sub>1</sub>-symmetric *trans*-X geometry observed in the solid state, fast ring inversion has to be present to result in the observed (apparent) C<sub>2</sub>-symmetry of the NMR spectra.) While the equivalence of the xylyl methyl resonances is thus a further indication of fast isomerisation of the complex geometry, the existence of two distinct xylyl methyl peaks in **3–6** unfortunately does not indicate the absence of these isomerisations.

To further investigate the possibility of a fast isomerisation, proton NMR spectra of **5** were recorded at variable temperatures down to –50 °C. While no splitting of resonances was observed, significant broadening of all resonances occurred below –20 °C, indicative of a dynamic process (Fig. 6 and ESI†). In summary, while there is thus no clear evidence for dynamic processes in **3–6**, the available data indicate that a fast isomerisation is indeed present. Given that isomers **A** and **C** were observed in the solid state, it seems reasonable to presume that the complexes retain the geometry observed in the solid state and that a *cis*-*trans* isomerisation is responsible for the peak broadening at low temperatures, without necessarily forming the wrong stereomatch **B** or C<sub>1</sub>-symmetric species **D**.



Scheme 6

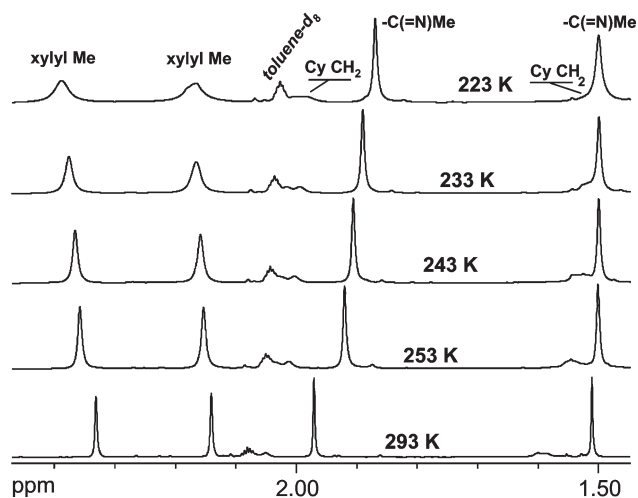


Fig. 6  $^1\text{H}$  NMR spectra (aliphatic region) of **5** at different temperatures. See ESI† for complete spectra.

### Lactide polymerization

Attempts to obtain a cationic alkoxide complex  $[\text{C}_6\text{H}_{10}(\text{nacnac}^{\text{Xyl}})_2\text{ZrOEt}]^+$ , which would be an attractive catalyst for lactide polymerization, from the reaction of **5** with either *para*-toluenesulfonic acid, triflic acid or  $[\text{PhN}(\text{H})\text{Me}_2][\text{OTf}]$  under a variety of conditions yielded only complex product mixtures, in which the protonated ligand was the most prevalent species. The reaction of **4** with one equiv. of  $\text{AgOTf}$ , followed by the reaction with  $\text{NaOEt}$ , likewise did not afford the desired cationic complex. We thus investigated octahedrally coordinated **5** directly as a catalyst for lactide polymerization. While six-coordinate zirconium alkoxide complexes have been shown to be active for lactide polymerization, they typically display only moderate activity, requiring several hours at temperatures of  $>70^\circ\text{C}$  in solution<sup>31–34</sup> or polymerization in a molten polymer,<sup>35–37</sup> which is not surprising for a sterically saturated octahedral complex. We were thus surprised to note that *rac*-lactide polymerization with **5** at room temperature in a dichloromethane solution reached 40% conversion already after one minute. Conversion did not exceed 50%, however, indicative of catalyst decomposition in this solvent (see ESI†). Better catalyst stability was obtained in toluene or diethyl ether, but the lactide monomer has only limited solubility in these solvents. Polymerization in THF finally led to fast and complete (95%) conversion of the monomer in 5 min (see ESI†). For comparison, the unbridged bisdiketiminato complex  $\text{nacnac}^{\text{Bn}}_2\text{Zr}(\text{OEt})_2$  was only reactive in the molten monomer at  $130^\circ\text{C}$  and still required 30 min to reach  $>95\%$  conversion.<sup>23</sup> As observed for the substitution of chloride ligands in **4**, bridging of the diketiminates thus drastically increased the reactivity of the complex.

More detailed investigations of the reaction kinetics showed the expected first-order dependence on monomer concentration (Fig. 7). Reactions typically reached completion in less than 5 min, but conversions did not exceed  $\approx 95\%$ . Incomplete conversion is typical for lactide polymerizations and attributed to a reversible polymerization.<sup>38,39</sup> Apparent rate constants at catalyst concentrations of 0.5–2 mM show a linear dependence on

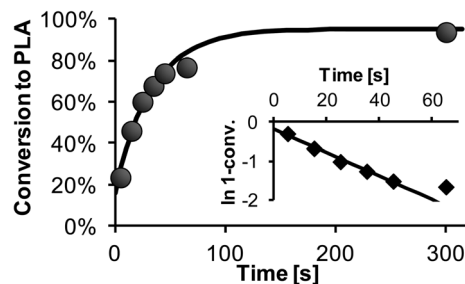


Fig. 7 PLA concentration vs. time for *rac*-lactide polymerization with **5**:  $[\text{lactide}] = 0.6\text{ M}$ ;  $[\mathbf{5}] = 2\text{ mM}$ ; THF; ambient temperature. The inset shows the linearised plot of monomer consumption assuming a first-order rate law;  $k_{\text{obs}} = 0.030\text{ s}^{-1}$ .

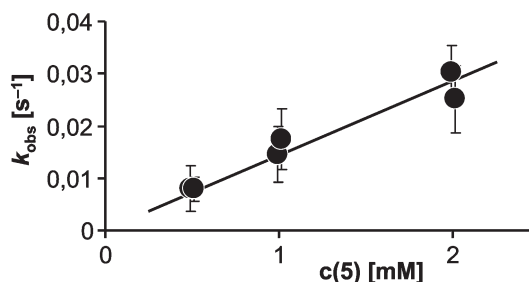


Fig. 8 Dependence of apparent rate constants  $k_{\text{obs}}$  on catalyst concentration;  $k = 14(1)\text{ L mol}^{-1}\text{ s}^{-1}$ .

catalyst concentration (Fig. 8), yielding a second-order rate constant at room temperature of  $k_{298\text{ K}} = 14(1)\text{ L mol}^{-1}\text{ s}^{-1}$ . To the best of our knowledge, this is the highest activity, by several orders of magnitude, reported for any zirconium or other group 4 complexes in lactide polymerization. Highly active Zr catalysts include a salalen Zr complex, described as “incredibly active” and which reached 99% conversion in 6 h ( $k_{298\text{ K}} \approx 5 \times 10^{-2}\text{ L mol}^{-1}\text{ s}^{-1}$ ),<sup>40</sup> a carbene Zr complex (95% after 15 h,  $k_{298\text{ K}} \approx 5 \times 10^{-3}\text{ L mol}^{-1}\text{ s}^{-1}$ ),<sup>41</sup> a sulfonamide Zr complex (5 h at  $60^\circ\text{C}$  to reach completion,  $k_{333\text{ K}} \approx 1 \times 10^{-2}\text{ L mol}^{-1}\text{ s}^{-1}$ ),<sup>42</sup> and a dithiolate Hf complex reported in 2010 to show the “highest activity of any group 4 metal catalyst”, which reached complete conversion in 1 min in a molten monomer ( $k_{403\text{ K}} \approx 4\text{ L mol}^{-1}\text{ s}^{-1}$ ).

While **5** thus displays an extremely high activity for group 4 complexes and compares well with the most active catalyst systems reported so far for the polymerization of lactide, its remaining characteristics, such as stereoselectivity, complex stability and polymer molecular weight control, are much less desirable. *Stereoselectivity*: all obtained polymers are essentially atactic with a slight heterotactic bias ( $P_r = 0.56\text{--}0.64$ ). The lack of isoselectivity imposed by the  $C_2$ -symmetric complex might be due to thermodynamic, kinetic or mechanistic reasons: (i) in the crystal structure of **3** and **5** we note that the introduction of the bridge forces the central atom of the diketiminato ligand (**3**: Fig. 1, C12; **5**: Fig. 3, C6/C36) towards the ancillary ligands, occupying the “empty” part of the catalytic pocket. (ii) The observed dynamic process in the NMR might prevent stereochemical stability of the catalytic site. (iii) The active species might not be a  $C_2$ -symmetric *cis*-isomer, but rather a species for which

less stereocontrol by the chiral bridge would be expected, such as the *trans*-isomer or a tetracoordinated species (Scheme 6).

**Complex stability:** despite rigorous drying of solvents and repeated recrystallisation of lactide, the stability of **5** under polymerization conditions is limited. All kinetic analyses show slight deviations from first order behaviour, which can be ascribed to catalyst decomposition. No further polymerization is observed, when a second portion of lactide is added after 15 min polymerization time. In fact, polymerizations either reached completion in less than 5 min or, in the case of lower activities, such as with catalyst concentrations below 0.5 mM, did not reach completion at all.

**Polymer molecular weight.** Resulting polymers showed broad, sometimes bimodal polymer molecular weight distributions with polymer molecular weights much lower than expected even for two chains produced per zirconium center and despite high conversions of >90%. Polymerizations in solvents other than THF or at different lactide : Zr ratios yielded the same results (see ESI†). The obtained polymers contained a sizeable fraction of oligomers with polymerization degrees lower than 10. Maldi-MS analysis of the oligomeric fraction showed a series of peaks with  $m/z$  ratios of  $n \cdot 72 + m(\text{Na}^+)$  (Fig. 9). Combined with the overall to high number of polymer chains per catalyst, this indicates that intramolecular transesterification leads to the formation of cyclic oligomers next to linear polymers.

Intrigued by the variations of activity on aging of catalyst stock solutions, as well as by the unusual high activity of **5** in general, we investigated the effects of potential contaminants on polymerization activity. Due to the possibility of fast alkoxide exchange, the observed polymer molecular weights do not exclude that small quantities of a highly active species are responsible for the observed polymerization activity. Polymerizations using possible contaminants from the catalyst preparation, *i.e.* free ligand **2H**<sub>2</sub>, sodium ethoxide, ZrCl<sub>4</sub>(THF)<sub>2</sub> or

combinations thereof, as an initiator did not result in any activity of the same order of magnitude as the activity observed for **5** (see ESI†). Although these polymerizations were not investigated in detail, it should be noted that sodium ethoxide in the presence of free ligand **2H**<sub>2</sub> showed surprisingly high activities (94% conversion in 1 h at ambient temperature).

In an alternative approach, we added selected contaminants to *rac*-lactide polymerizations with **5**<sub>slow</sub>, *i.e.* stock solutions of **5** which showed less than the normally observed activity (approximately 20–35% of the maximum activity observed, *cf.* Table S3†). Surprisingly, addition of protic contaminants, such as water or *para*-toluenesulfonic acid, slightly *increased* the polymerization activity of **5**<sub>slow</sub>, albeit never surpassing the maximum activity observed for **5**. Addition of lactic acid quenched the polymerization (Table S3†). While the slight rate-enhancing effect of water remains unexplained at the moment, it seems improbable that activation by protic substances is responsible for the high activities observed (see ESI†). Water (or TsOH) might rather be involved in the re-activation of deactivated species, for example after the reaction with lactic acid impurities, although no mechanism for this can be proposed at the moment.

## Conclusion

Bridging of two diketiminate ligands by a cyclohexanediyl bridge increased, as intended, the reactivity of bisdiketiminate zirconium complexes, which are now able to undergo ligand exchange and show vastly higher activities in lactide polymerization. The chiral bridge also shows a clear stereochemical impact on the conformation at the metal center. Unfortunately, the steric constraints introduced permit the formation of undesired *trans*-X<sub>2</sub> species and variable temperature NMR spectra showed evidence for a dynamic process, which is most likely a fast

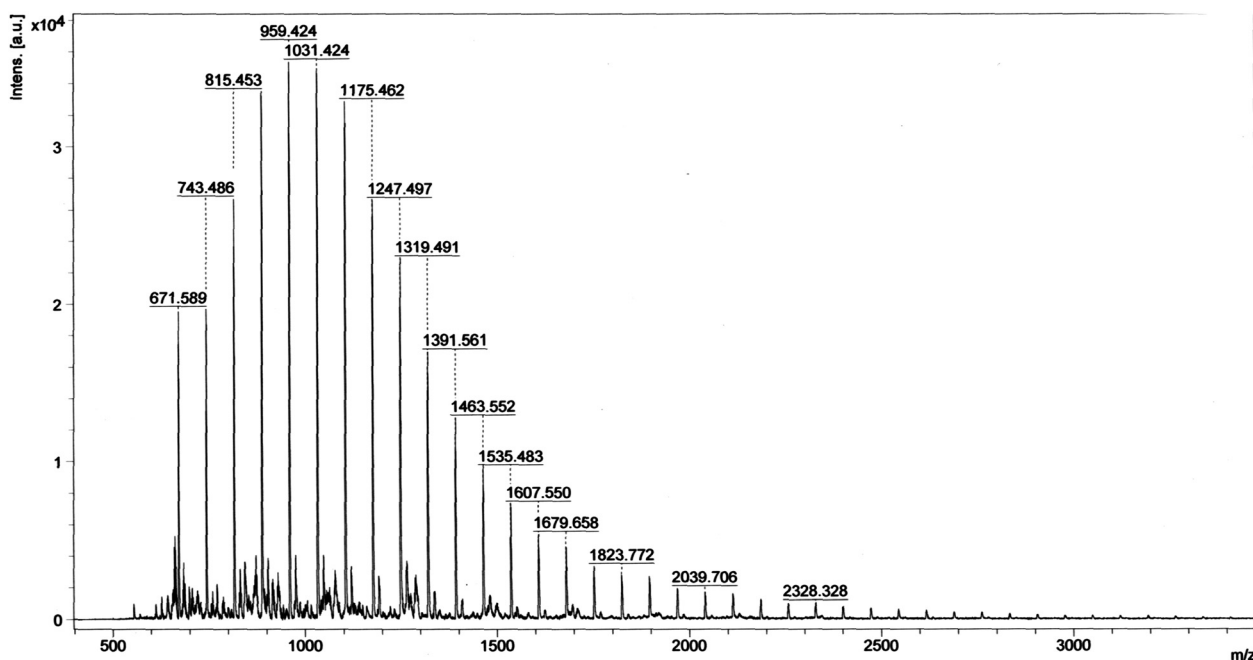


Fig. 9 Maldi-mass spectrum of the oligomeric fraction of PLA obtained from **5** (2 mM, THF, [lactide]/[**5**] = 100/1).

isomerisation between *cis*- and *trans*-X<sub>2</sub> complexes. In lactide polymerization, the unprecedented high activity of diethoxy complex **5** provides valuable starting points in optimizing group 4-based lactide polymerization catalysts. Its lack in stereoselectivity, its low stability under polymerization conditions, and the formation of notable amounts of cyclic oligomers drastically reduce its value as a catalyst for cyclic ester polymerizations, however. We are currently investigating other applications of the chiral C<sub>6</sub>H<sub>10</sub>(*nacnac*<sup>Xyl</sup>)<sub>2</sub>ZrX<sub>2</sub> system, in particular hydroamination and carbozirconation reactions.

## Experimental section

All reactions, except ligand synthesis, were carried out using Schlenk and glove box techniques under a nitrogen atmosphere. ZrCl<sub>4</sub>(THF)<sub>2</sub>,<sup>43</sup> Zr(NMe<sub>2</sub>)<sub>4</sub>,<sup>44</sup> and 4-[(2,6-dimethylphenyl)amino]-pent-3-en-2-one<sup>45</sup> were prepared according to literature procedures. ZrCl<sub>4</sub>, NaOEt, LiNMe<sub>2</sub> and other chemicals were purchased from common commercial suppliers. <sup>1</sup>H and <sup>13</sup>C NMR spectra were acquired on a Bruker AMX 400 or Bruker AV 400 spectrometer. <sup>19</sup>F NMR spectra were acquired on a Bruker AV 400 spectrometer. Chemical shifts were referenced to the residual signals of the deuterated solvents (C<sub>6</sub>D<sub>6</sub>: <sup>1</sup>H: δ 7.16 ppm, <sup>13</sup>C: δ 128.38 ppm; CDCl<sub>3</sub>: <sup>1</sup>H: δ 7.26 ppm, <sup>13</sup>C: δ 77.00 ppm). Solvents were dried by passage through activated aluminum oxide (MBraun SPS) and de-oxygenated by repeated extraction with nitrogen. Polymerization solvents were additionally passed through a column of activated molecular sieves. C<sub>6</sub>D<sub>6</sub> was dried over sodium, CDCl<sub>3</sub> was dried over CaH<sub>2</sub> and both were distilled under reduced pressure, and then degassed by three freeze–pump–thaw cycles. Racemic lactide was sublimed and recrystallized twice from dry ethyl acetate. Elemental analyses were performed by the Laboratoire d'analyse élémentaire (Université de Montréal).

## X-ray diffraction studies

Diffraction data were collected on a Bruker Smart 6000 with Helios MX mirror optics and Cu Kα radiation (rotating anode), using the APEX2 software package.<sup>46</sup> Data reduction was performed with SAINT,<sup>47</sup> absorption corrections with SADABS.<sup>48</sup> Structures were solved with direct methods (SHELXS97).<sup>49</sup> All non-hydrogen atoms were refined anisotropically using full-matrix least-squares on *F*<sup>2</sup> and hydrogen atoms refined with fixed isotropic *U* using a riding model (SHELXL97).<sup>49</sup> One ethyl group in **5** was disordered and refined anisotropically with refined occupation factors of 0.73 and 0.27. The cyclohexanediamine bridge in **6** was found to be disordered and was refined, partially isotropically, with appropriate restraints. For further details, please see Table 2 or the ESI.†

(±)-C<sub>6</sub>H<sub>10</sub>(*nacnac*<sup>Xyl</sup>)<sub>2</sub>H<sub>2</sub>, **2H<sub>2</sub>**. [Me<sub>3</sub>O][BF<sub>4</sub>] (1.08 g, 7.3 mmol) was added to a yellow dichloromethane solution of 4-[(2,6-dimethylphenyl)amino]-pent-3-en-2-one (1.49 g, 7.3 mmol, 10 mL). The resulting suspension was stirred for approximately 2 h until complete dissolution of [Me<sub>3</sub>O][BF<sub>4</sub>]. A dichloromethane solution of (±)-*trans*-cyclohexane-1,2-diamine (0.21 g, 1.8 mmol, 1.0 mL) was added, after which stirring was continued for 30 min to yield an orange solution. A mixture of (±)-*trans*-cyclohexane-1,2-diamine (0.24 mL, 1.8 mmol) and triethylamine (0.76 mL, 5.4 mmol) was added. After short additional stirring (5 min), the volatiles were removed *in vacuo*. Diethyl ether (100 mL) was added to the residue. The obtained suspension was treated with an excess of Et<sub>3</sub>N (0.11 mol, 15 mL) and stirred for 5 min. From the yellow phase separated by decantation, solvents were removed *in vacuo* and the residual yellow solid was crystallized from ethanol at –20 °C to afford 1.35 g (76%) of yellow crystals.

<sup>1</sup>H NMR (CDCl<sub>3</sub>, 400 MHz): δ 10.94 (bs, 2H, NH), 7.01 (d, *J* = 2 Hz, 4H, *meta* Ar), 6.85 (t, *J* = 2 Hz, 2H, *para* Ar), 4.56 (bs, 2H, CH(C=O)), 3.14 (m, 2H, Cy CH), 2.17 (s, 6H, Me<sub>2</sub>Ar),

**Table 2** Details of X-ray diffraction studies

	<b>3</b>	<b>4</b>	<b>5</b>	<b>6</b>
Formula	C <sub>36</sub> H <sub>54</sub> N <sub>6</sub> Zr	C <sub>32</sub> H <sub>42</sub> Cl <sub>2</sub> N <sub>4</sub> Zr·C <sub>6</sub> H <sub>6</sub>	C <sub>36</sub> H <sub>52</sub> N <sub>4</sub> O <sub>2</sub> Zr	C <sub>34</sub> H <sub>48</sub> N <sub>4</sub> Zr
<i>M<sub>w</sub></i> (g mol <sup>-1</sup> ); <i>d<sub>calcd</sub></i> (g cm <sup>-3</sup> )	662.07; 1.27	722.92; 1.33	664.04; 1.27	603.98; 1.26
Crystal size (mm)	0.14 × 0.14 × 0.18	0.03 × 0.03 × 0.08	0.08 × 0.08 × 0.08	0.1 × 0.1 × 0.3
<i>T</i> (K); <i>F</i> (000)	200; 1408	150; 756	150; 704	150; 1280
Crystal system	Monoclinic	Triclinic	Triclinic	Monoclinic
Space group	<i>C</i> 2/ <i>c</i>	<i>P</i> $\bar{1}$	<i>P</i> $\bar{1}$	<i>P</i> 2 <sub>1</sub> / <i>n</i>
Unit cell:				
<i>a</i> (Å)	18.5065(3)	9.7217(4)	10.9326(11)	11.4759(9)
<i>b</i> (Å)	11.7278(2)	11.9708(5)	11.2187(12)	14.9142(12)
<i>c</i> (Å)	17.2506(4)	16.5433(7)	16.3787(16)	18.6288(14)
$\alpha$ (°)		100.423(2)	82.459(5)	
$\beta$ (°)	112.842(1)	104.614(2)	71.522(5)	91.042(3)
$\gamma$ (°)		96.408(2)	65.213(5)	
<i>V</i> (Å <sup>3</sup> ); <i>Z</i>	3450.5(1); 4	1807.0(1); 2	1729.7(3); 2	3187.9(4); 4
$\theta$ range (°); completeness	4.6–72.6; 0.99	2.8–69.6; 0.97	2.8–69.7; 0.98	3.8–69.8; 1.00
Collected reflections; <i>R<sub>c</sub></i>	22047; 0.014	25219; 0.060	66389; 0.032	116139; 0.024
Unique reflections; <i>R<sub>int</sub></i>	3393; 0.031	6640; 0.049	6426; 0.084	5989; 0.083
$\mu$ (mm <sup>-1</sup> ); abs. corr.	2.85; multi-scan	4.09; multi-scan	2.88; multi-scan	3.02; multi-scan
<i>R<sub>1</sub></i> ( <i>F</i> ); <i>wR</i> ( <i>F</i> <sup>2</sup> ) ( <i>I</i> > 2σ( <i>I</i> ))	0.027; 0.073	0.033; 0.070	0.037; 0.096	0.045; 0.117
<i>R<sub>1</sub></i> ( <i>F</i> ); <i>wR</i> ( <i>F</i> <sup>2</sup> ) (all data)	0.027; 0.073	0.047; 0.073	0.039; 0.102	0.047; 0.118
GoF( <i>F</i> <sup>2</sup> )	1.098	0.915	1.107	1.156
Residual electron density	0.36, –0.41	0.58, –0.34	0.97; –0.58	1.39; –0.68

2.04 (s, 6H,  $Me_2Ar$ ), 2.02 (s, 6H,  $Me(C=N)$ ), 1.95–1.86 (m, 8H,  $CH_2$ ), 1.59 (s, 6H,  $Me(C=N)$ ).  $^{13}C\{^1H\}$  NMR ( $CDCl_3$ , 101 MHz):  $\delta$  165.9 ( $MeC=N$ ), 155.2 ( $MeC=N$ ), 149.5 (*ipso* Ar), 128.1 (Ar), 127.7 (Ar), 127.6 (Ar), 127.5 (Ar), 121.7 (*para* Ar), 92.6 ( $CH(C=N)$ ), 58.0 (Cy CH), 33.5 (Cy  $CH_2$ ), 24.7 (Cy  $CH_2$ ), 21.2 ( $MeC=N$ ), 19.6 ( $MeC=N$ ), 18.5 ( $Me_2Ar$ ), 18.2 ( $Me_2Ar$ ).  $^1H$  NMR ( $C_6D_6$ , 400 MHz):  $\delta$  11.09 (bs, 2H, NH), 7.10 (d,  $J = 2$  Hz, 4H, *meta* Ar), 6.96 (t,  $J = 2$  Hz, 2H, *para* Ar), 4.61 (bs, 2H,  $CH(C=N)$ ), 2.90 (m, 2H, Cy CH), 2.20 (s, 6H,  $Me_2Ar$ ), 2.17 (s, 6H,  $Me_2Ar$ ), 1.87 (s, 6H,  $Me(C=N)$ ), 1.67 (m, 2H, Cy  $CH_2$ ), 1.58 (s, 6H,  $Me(C=N)$ ) 1.3–0.80 (m, 6H, Cy  $CH_2$ ).  $^{13}C\{^1H\}$  NMR ( $C_6D_6$ , 101 MHz):  $\delta$  166.2 ( $MeC=N$ ), 155.2 ( $MeC=N$ ), 150.3 (*ipso* Ar), 128.3 (Ar), 128.2 (Ar), 128.1 (Ar), 127.9 (Ar), 122.5 (*para* Ar), 93.6 ( $CH(C=N)$ ), 58.2 (Cy CH), 33.6 (Cy  $CH_2$ ), 24.6 (Cy  $CH_2$ ), 21.3 ( $MeC=N$ ), 19.7 ( $MeC=N$ ), 18.8 ( $Me_2Ar$ ), 18.7 ( $Me_2Ar$ ). Anal. calcd for  $C_{13}H_{26}N_2$ : C, 79.29; H, 9.15; N, 11.56; found C, 79.05; H, 9.18; N, 11.56.

**( $\pm$ )- $C_6H_{10}(nacnac^{Xyl}Li(THF))_2 \cdot 0.5$  THF,  $2Li_2(THF)_2 \cdot 0.5$  THF.** To a yellow THF solution of ligand **1a** (0.3 g, 0.63 mmol), *n*BuLi (2.9 M, 0.43 mL, 0.13 mmol) was added gradually at room temperature. The obtained orange solution was stirred for 5 min. All volatiles were removed *in vacuo* to give an orange oil. Addition of hexanes (5 mL) gave an off-white precipitate, which was isolated by decantation and dried under vacuum to yield an off-white powder (0.32 g, 80%).

$^1H$  NMR ( $C_6D_6$ , 400 MHz):  $\delta$  7.10 (d,  $J = 2$  Hz, 2H, *meta* Ar), 7.03 (d,  $J = 2$  Hz, 2H, *meta* Ar), 6.90 (t,  $J = 2$  Hz, 2H, *para* Ar), 4.67 (bs, 2H,  $CH(C=N)$ ), 3.40 (m, 10H, THF), 3.29 (m, 2H, Cy CH), 2.32 (s, 6H,  $Me_2Ar$ ), 2.17 (s, 6H,  $Me_2Ar$ ), 2.12 (m, 2H, Cy  $CH_2$ ), 1.99 (s, 6H,  $Me(C=N)$ ), 1.78 (s, 6H,  $Me(C=N)$ ), 1.40–1.32 (m, 6H, Cy  $CH_2$ ), 1.14 (m, 10H, THF).  $^{13}C\{^1H\}$  NMR ( $C_6D_6$ , 101 MHz):  $\delta$  164.5 ( $MeC=N$ ), 161.8 ( $MeC=N$ ), 153.6 (*ipso* Ar), 131.2 (*ortho* Ar), 130.7 (*ortho* Ar), 128.13 (*meta* Ar), 127.8 (*meta* Ar), 121.4 (*para* Ar), 93.5 ( $CH(C=N)$ ), 68.3 (THF), 65.9 (Cy CH), 35.9, 19.6 (Cy  $CH_2$ ), 26.5, 23.0 ( $MeC=N$ ), 25.2 (THF), 19.6 ( $Me_2Ar$ ), 19.0 ( $Me_2Ar$ ). Anal. calcd for  $C_{40}H_{58}Li_2N_4O_2 \cdot 0.5$   $C_4H_8O$ : C, 74.53; H, 9.23; N, 8.28; found C, 74.14; H, 9.22; N, 8.68. (NMR shows the presence of 2.5 THF).

**( $\pm$ )- $C_6H_{10}(nacnac^{Xyl})_2Zr(NMe_2)_2$ , **3**.**  $Zr(NMe_2)_4$  (0.14 g, 0.53 mmol) and ligand  $2H_2$  (0.25 g, 0.53 mmol) were mixed and heated, in the absence of a solvent, to 120 °C under a  $N_2$  atmosphere for 1 h. The obtained brown oil was dissolved in toluene (1 mL) and crystallized by slow evaporation at room temperature (0.25 g, 71%).

$^1H$  NMR ( $C_6D_6$ , 400 MHz):  $\delta$  7.10 (d,  $J = 2$  Hz, 2H, *meta* Ar), 7.00 (d,  $J = 2$  Hz, 2H, *meta* Ar), 6.93 (t,  $J = 2$  Hz, 2H, *p*-Ar), 5.04 (bs, 2H,  $CH(C=N)$ ), 3.79 (m, 2H, Cy CH), 2.80 (s, 6H,  $NMe_2$ ), 2.50 (s, 6H,  $Me_2Ar$ ), 2.13 (m, 2H, Cy  $CH_2$ ), 2.09 (s, 6H,  $Me_2Ar$ ), 1.90 (s, 6H,  $Me(C=N)$ ), 1.77 (s, 6H,  $NMe_2$ ), 1.58 (s, 2H, Cy  $CH_2$ ), 1.56 (s, 6H,  $Me(C=N)$ ), 1.29–1.25 (m, 4H, Cy  $CH_2$ ).  $^{13}C\{^1H\}$  NMR ( $C_6D_6$ , 101 MHz):  $\delta$  166.1 ( $Me(C=N)$ ), 163.0 ( $Me(C=N)$ ), 153.7 (*ipso* Ar), 132.1 (*ortho* Ar), 131.9 (*ortho* Ar), 128.7 (*meta* Ar), 127.7 (*meta* Ar), 123.7 (*para* Ar), 105.7 ( $CH(C=N)$ ), 70.2 (Cy CH), 43.2 (Cy  $CH_2$ ), 41.5 (Cy  $CH_2$ ), 35.3 ( $NMe_2$ ), 25.7 ( $NMe_2$ ), 24.8 ( $Me(C=N)$ ), 22.6 ( $Me$

( $C=N$ ), 21.3 ( $Me_2Ar$ ), 18.9 ( $Me_2Ar$ ). Anal. calcd for  $C_{36}H_{54}N_6Zr$ : C, 65.31; H, 8.22; N, 12.69; found C, 64.68; H, 8.86; N, 12.42.

**( $\pm$ )- $C_6H_{10}(nacnac^{Xyl})_2ZrCl_2$ , **4**.** A suspension of  $ZrCl_4(THF)_2$  (0.50 g, 1.34 mmol) in toluene (10 mL) was added drop by drop to a solution of  $2Li_2(THF)_2 \cdot 0.5$  THF (0.86 g, 1.34 mmol) in toluene (10 mL) while stirring. After 10 min at room temperature, the yellow suspension obtained was filtered and the remaining residue extracted with toluene (5 mL). The toluene solution was evaporated to dryness yielding a yellow powder (0.69 g, 80%). Crystals suitable for elemental analysis and X-ray structure determination were obtained by slow evaporation of  $C_6D_6$ .

$^1H$  NMR ( $CDCl_3$ , 400 MHz):  $\delta$  6.94–6.85 (m, 6H, Ar), 5.45 (bs, 2H,  $CH(C=N)$ ), 4.19 (m, 2H, Cy CH), 2.18 (s, 6H,  $Me(C=N)$ ), 2.14 (s, 6H,  $Me_2Ar$ ), 2.11 (m, 2H, Cy  $CH_2$ ), 2.06 (s, 6H,  $Me_2Ar$ ), 1.87–1.72 (m, 4H, Cy  $CH_2$ ), 1.64 (s, 6H,  $Me(C=N)$ ), 1.41 (m, 2H, Cy  $CH_2$ ).  $^1H$  NMR ( $C_6D_6$ , 400 MHz):  $\delta$  6.95–6.84 (m, 6H, Ar), 5.39 (bs, 2H,  $CH(C=N)$ ), 4.19 (m, 2H, Cy CH), 2.37 (s, 6H,  $Me_2Ar$ ), 2.29 (s, 6H,  $Me_2Ar$ ), 1.86 (m, 2H, Cy  $CH_2$ ), 1.83 (s, 6H,  $Me(C=N)$ ), 1.56 (s, 6H,  $Me(C=N)$ ), 1.53–1.46 (m, 4H, Cy  $CH_2$ ), 1.03 (m, 2H, Cy  $CH_2$ ).  $^{13}C\{^1H\}$  NMR ( $C_6D_6$ , 101 MHz):  $\delta$  66.2 ( $MeC=N$ ), 161.2 ( $MeC=N$ ), 133.1 (*ortho* Ar), 132.6 (*ortho* Ar), 128.5 (*ipso* Ar), 128.4 (*meta* Ar), 128.3 (*meta* Ar), 125.1 (*para* Ar), 105.7 ( $CH(C=N)$ ), 69.0 (Cy CH), 32.6 (Cy  $CH_2$ ), 25.3 ( $MeC=N$ ), 23.3 ( $MeC=N$ ), 22.5 ( $Me_2Ar$ ), 19.6 ( $Me_2Ar$ ), 19.53 (Cy  $CH_2$ ). Anal. calcd for  $C_{32}H_{42}N_4ZrCl_2 \cdot C_6D_6$ : C, 62.61; H, 6.64; N, 7.69; found C, 62.79; H, 6.94; N, 7.57 (X-ray structure shows the presence of one  $C_6D_6$ ).

**( $\pm$ )- $C_6H_{10}(nacnac^{Xyl})_2Zr(OEt)_2$ , **5**.** Method A: a yellow solution of **4** (0.32 g, 0.50 mmol) in toluene (10 mL) was added drop by drop to a suspension of NaOEt (0.86 g, 1.34 mmol) in toluene (5 mL). The obtained red suspension was refluxed for 3 days. The suspension was filtered while hot and the obtained filtrate was evaporated to dryness to yield a red oil (0.30 g, 91%, 90% purity determined by NMR). Addition of hexane (2 mL) gave a red solution which yielded orange crystals separated upon standing (200 mg, 60%).

Method B: to a suspension of  $ZrCl_4(THF)_2$  (222 mg, 0.59 mmol) in toluene (5 mL) was added a suspension of NaOEt (80 mg, 1.2 mmol) in toluene (20 mL). The suspension was heated for 3 h at 80 °C. The resulting mixture was added to a solution of  $2Li_2THF_2$  (400 mg, 0.59 mmol) in toluene (10 mL). The orange suspension was heated overnight at 80 °C, then filtered. Recrystallisation of the residue yielded **5** as orange crystals (55%).

$^1H$  NMR ( $C_6D_6$ , 400 MHz):  $\delta$  7.06 (d,  $J = 8$  Hz, 2H, *meta* Ar), 7.04 (d,  $J = 8$  Hz, 2H, *meta* Ar), 6.93 (t,  $J = 8$  Hz, 2H, *para* Ar), 5.10 (bs, 2H,  $CH(C=N)$ ), 3.75 (m, 2H, Cy CH), 3.20 (m, 4H,  $OCH_2$ ), 2.37 (s, 6H,  $Me_2Ar$ ), 2.20 (s, 6H,  $Me_2Ar$ ), 2.07 (m, 2H, Cy  $CH_2$ ), 1.96 (s, 6H,  $Me(C=N)$ ), 1.55–1.48 (m, 8H, Cy CH &  $Me(C=N)$ ), 1.30 (m, 4H, Cy  $CH_2$ ), 0.77 (t,  $J = 7$  Hz, 6H,  $OCH_2Me$ ).  $^{13}C\{^1H\}$  NMR ( $C_6D_6$ , 101 MHz):  $\delta$  63.8 ( $MeC=N$ ), 162.8 ( $MeC=N$ ), 152.8 (*ipso* Ar), 132.6 (*ortho* Ar), 130.9 (*ortho* Ar), 128.6 (*meta* Ar), 127.9 (*meta* Ar), 123.9 (*para* Ar), 104.1 ( $CH(C=N)$ ), 68.8 (Cy CH), 63.8 ( $OCH_2Me$ ), 34.8 (Cy  $CH_2$ ), 25.8 ( $OCH_2Me$ ), 22.7 ( $Me_2Ar$ ), 22.3 (Cy  $CH_2$ ), 19.7

( $Me_2Ar$ ), 19.2 ( $Me(C=N)$ ), 19.0 ( $Me(C=N)$ ). Anal. calcd for  $C_{36}H_{52}N_4O_2Zr$ : C, 65.11; H, 7.89; N, 8.44; found C, 64.92; H, 8.04; N, 8.14.

( $\pm$ )- $C_6H_{10}(nacnac^{Xyl})_2ZrMe_2 \cdot 0.5$  toluene, **6**. A mixture of MeLi (10 mg, 0.45 mmol) in toluene (2 mL) and  $AlMe_3$  in hexane (0.20 M, 0.12 mL, 0.024 mmol) was gradually added at  $-78$  °C to a solution of **4** (150 mg, 0.23 mmol) in toluene (10 mL) and stirred for 5 min. The cold bath was removed and stirring was completed in another 5 min. The obtained yellow suspension was filtered cold and the remaining residue was extracted with toluene (5 mL). The combined toluene filtrates were concentrated to 2 mL. Slow diffusion of hexane into a toluene solution of **6** at  $-35$  °C gave yellow crystals (50 mg, 36%).  $^1H$  NMR of the obtained crystals showed the presence of 0.5 equiv. of toluene.

$^1H$  NMR ( $C_6D_6$ , 400 MHz):  $\delta$  7.10–6.93 (m, 6H, Ar), 5.27 (bs, 2H,  $CH(C=N)$ ), 3.69 (m, 2H, Cy CH), 2.34 (s, 6H,  $Me_2Ar$ ), 2.29 (s, 6H,  $Me_2Ar$ ), 2.07–1.93 (m, 4H, Cy  $CH_2$ ), 1.86 (s, 6H,  $Me(C=N)$ ), 1.66 (s, 6H,  $Me(C=N)$ ), 1.50 (m, 2H, Cy  $CH_2$ ), 1.04 (m, 2H, Cy  $CH_2$ ),  $-0.06$  (s, 6H, ZrMe).  $^{13}C$  NMR ( $C_6D_6$ , 101 MHz):  $\delta$  164.0, 156.2 ( $Me(C=N)$ ), 153.1 (*ipso* Ar), 132.2 (*ortho* Ar), 131.7 (*ortho* Ar), 129.6 (*meta* Ar), 128.8 (*meta* Ar), 124.7 (*para* Ar), 103.8 ( $CH(C=N)$ ), 67.4 (Cy CH), 57.7, 33.9 (Cy  $CH_2$ ), 26.0 ( $Me_2Ar$ ), 23.9 ( $Me_2Ar$ ), 22.7 ( $Me(C=N)$ ), 19.9 ( $Me(C=N)$ ), 19.8 (ZrMe). Anal. calcd for  $C_{34}H_{48}N_4Zr \cdot \frac{1}{2}C_7H_8$ . C, 69.29; H, 8.06; N, 8.62; found C, 68.87; H, 8.22; N, 8.26.

### rac-Lactide polymerization

In a well closed vial, a toluene solution of **5** (200  $\mu$ L, 10 mM, 2.0 mmol) was added to a THF solution of *rac*-lactide (87 mg, 0.60 mmol, 0.8 mL). Reaction mixtures were quenched at the desired polymerization time by addition of a dichloromethane solution of acetic acid (5 mM). Samples for kinetic investigations were taken at the desired intervals and added to vials already containing a dichloromethane solution of acetic acid (5 mM). In both cases, volatiles were immediately evaporated afterwards. Solid polymer samples were stored at  $-80$  °C. Conversion was determined from  $^1H$  NMR in  $CDCl_3$  by comparison to remaining lactide.  $P_r$  values were determined from homo-decoupled  $^1H$  NMR spectra. Molecular weight analyses were performed on a Waters 1525 gel permeation chromatograph equipped with three Phenomenex columns and a refractive index detector at 35 °C. THF was used as the eluent at a flow rate of 1.0 mL  $min^{-1}$  and polystyrene standards (Sigma-Aldrich, 1.5 mg  $mL^{-1}$ , prepared and filtered (0.2 mm) directly prior to injection) were used for calibration. Obtained molecular weights were corrected by a Mark–Houwink factor of 0.58.<sup>50</sup> Mass spectroscopic analyses were performed on a MALDI TOF/TOF Ultraflex extreme mass spectrometer equipped with a SmartBeam II Nd:YAG/355 nm laser operating at 1 kHz and providing a laser focus down to 20  $\mu$ m in diameter for the “minimum” focus setting (Bruker Daltonics, Billerica, MA). The matrix used contained 10 mg  $mL^{-1}$  of 2,5-dihydroxybenzoic acid (DHB) in MeOH : deionised water (1 : 1).

### Acknowledgements

Floriane Cuenca and Arnaud Parrot contributed during their internship to the work presented here. We thank Sylvie Bilodeau for variable temperature NMR measurements, Erik Fournaise for MS measurements and Francine Bélanger for help with X-ray crystallography. I. E. and T. W. received a doctoral stipend from the Fonds de recherche du Québec – Nature et technologies (FQRNT). This work was supported by the Canadian National Research Council (NSERC) and the Centre in Green Chemistry and Catalysis (CGCC).

### References

- P. B. Hitchcock, M. F. Lappert and D.-S. Liu, *Chem. Commun.*, 1994, 2637–2638.
- B. Qian, W. J. Scanlon, M. R. Smith and D. H. Motry, *Organometallics*, 1999, **18**, 1693–1698.
- M. Rahim, N. J. Taylor, S. Xin and S. Collins, *Organometallics*, 1998, **17**, 1315–1323.
- L. Kakaliou, W. J. Scanlon, B. Qian, S. W. Baek, M. R. Smith and D. H. Motry, *Inorg. Chem.*, 1999, **38**, 5964–5977.
- R. Vollmerhaus, M. Rahim, R. Tomaszewski, S. Xin, N. J. Taylor and S. Collins, *Organometallics*, 2000, **19**, 2161–2169.
- X. Jin and B. M. Novak, *Macromolecules*, 2000, **33**, 6205–6207.
- F. Basuli, U. J. Kilgore, D. Brown, J. C. Huffman and D. J. Mindiola, *Organometallics*, 2004, **23**, 6166–6175.
- H. Hamaki, N. Takeda and N. Tokitoh, *Organometallics*, 2006, **25**, 2457–2464.
- R.-V. Fortuné, E. Verguet, P. O. Oguadinma and F. Schaper, *Acta Crystallogr. Struct. Rep. Online*, 2007, **63**, m2822–m2823.
- A. K. Mittal, A. Shukla, P. R. Shukla, A. K. Pathak and N. Ahmad, *Synth. React. Inorg. Met.-Org. Chem.*, 1995, **25**, 739–759.
- E. Shaviv, M. Botoshansky and M. S. Eisen, *J. Organomet. Chem.*, 2003, **683**, 165–180.
- R. Andrés, E. de Jesús, F. J. de la Mata, J. C. Flores and R. Gómez, *J. Organomet. Chem.*, 2005, **690**, 939–943.
- E. Verguet, R.-V. Fortuné, P. O. Oguadinma and F. Schaper, *Acta Crystallogr. Struct. Rep. Online*, 2007, **63**, m2539–m2540.
- E. Verguet, P. O. Oguadinma and F. Schaper, *Acta Crystallogr. Struct. Rep. Online*, 2007, **63**, m2541–m2542.
- A. R. Cabrera, Y. Schneider, M. Valderrama, R. Fröhlich, G. Kehr, G. Erker and R. S. Rojas, *Organometallics*, 2010, **29**, 6104–6110.
- R. S. Rojas, B. C. Peoples, A. R. Cabrera, M. Valderrama, R. Fröhlich, G. Kehr, G. Erker, T. Wiegand and H. Eckert, *Organometallics*, 2011, **30**, 6372–6382.
- R. S. Rojas, A. R. Cabrera, B. C. Peoples, K. Spannhoff, M. Valderrama, R. Fröhlich, G. Kehr and G. Erker, *Dalton Trans.*, 2012, **41**, 1243–1251.
- H. Hamaki, N. Takeda, M. Nabika and N. Tokitoh, *Macromolecules*, 2012, **45**, 1758–1769.
- I. El-Zoghbi, E. Verguet, P. O. Oguadinma and F. Schaper, *Inorg. Chem. Commun.*, 2010, **13**, 529–533.
- P. L. Franceschini, M. Morstein, H. Berke and H. W. Schmalle, *Inorg. Chem.*, 2003, **42**, 7273–7282.
- S. Gong, H. Ma and J. Huang, *J. Organomet. Chem.*, 2008, **693**, 3509–3518.
- S. Gong, H. Ma and J. Huang, *Dalton Trans.*, 2009, 8237–8247.
- I. El-Zoghbi, S. Latreche and F. Schaper, *Organometallics*, 2010, **29**, 1551–1559.
- L. Bourget-Merle, M. F. Lappert and J. R. Severn, *Chem. Rev.*, 2002, **102**, 3031–3066.
- I. El-Zoghbi, A. Ased, P. O. Oguadinma, E. Tchirioua and F. Schaper, *Can. J. Chem.*, 2010, **88**, 1040–1045.
- D. V. Vitanova, F. Hampel and K. C. Hultzs, *J. Organomet. Chem.*, 2005, **690**, 5182–5197.
- D. V. Vitanova, F. Hampel and K. C. Hultzs, *Dalton Trans.*, 2005, 1565–1566.
- D. V. Vitanova, F. Hampel and K. C. Hultzs, *J. Organomet. Chem.*, 2011, **696**, 321–330.

- 29 M. M. Melzer, S. Mossin, X. Dai, A. M. Bartell, P. Kapoor, K. Meyer and T. H. Warren, *Angew. Chem., Int. Ed.*, 2010, **49**, 904–907.
- 30 N. Carrera, N. Savjani, J. Simpson, D. L. Hughes and M. Bochmann, *Dalton Trans.*, 2011, **40**, 1016–1019.
- 31 A. L. Zelikoff, J. Kopilov, I. Goldberg, G. W. Coates and M. Kol, *Chem. Commun. (Cambridge, UK)*, 2009, 6804–6806.
- 32 J.-C. Buffet and J. Okuda, *Chem. Commun. (Cambridge, UK)*, 2011, **47**, 4796–4798.
- 33 S. L. Hancock, M. F. Mahon, G. Kociok-Köhn and M. D. Jones, *Eur. J. Inorg. Chem.*, 2011, **2011**, 4596–4602.
- 34 A. J. Chmura, D. M. Cousins, M. G. Davidson, M. D. Jones, M. D. Lunn and M. F. Mahon, *Dalton Trans.*, 2008, 1437–1443.
- 35 T. K. Saha, V. Ramkumar and D. Chakraborty, *Inorg. Chem.*, 2011, **50**, 2720–2722.
- 36 T. K. Saha, B. Rajashekhar and D. Chakraborty, *RSC Adv.*, 2012, **2**, 307–318.
- 37 T. K. Saha, B. Rajashekhar, R. R. Gowda, V. Ramkumar and D. Chakraborty, *Dalton Trans.*, 2010, **39**, 5091–5093.
- 38 A. Kowalski, A. Duda and S. Penczek, *Macromolecules*, 1998, **31**, 2114–2122.
- 39 J. Mosnáček, A. Duda, J. Libiszowski and S. Penczek, *Macromolecules*, 2005, **38**, 2027–2029.
- 40 E. L. Whitelaw, M. G. Davidson and M. D. Jones, *Chem. Commun. (Cambridge, UK)*, 2011, **47**, 10004–10006.
- 41 C. Romain, B. Heinrich, S. B. Laponnaz and S. Dagorne, *Chem. Commun. (Cambridge, UK)*, 2012, **48**, 2213–2215.
- 42 A. D. Schwarz, A. L. Thompson and P. Mountford, *Inorg. Chem.*, 2009, **48**, 10442–10454.
- 43 L. E. Manzer, *Inorg. Synth.*, 1982, **21**, 135–136.
- 44 D. C. Bradley and I. M. Thomas, *J. Chem. Soc.*, 1960, 3857.
- 45 J. Kim, J.-W. Hwang, Y. Kim, M. Hyung Lee, Y. Han and Y. Do, *J. Organomet. Chem.*, 2001, **620**, 1–7.
- 46 APEX2, Bruker AXS Inc., Madison, USA, 2006.
- 47 SAINT, Bruker AXS Inc., Madison, USA, 2006.
- 48 G. M. Sheldrick, *SADABS*, Bruker AXS Inc., Madison, USA, 1996 & 2004.
- 49 G. M. Sheldrick, *Acta Crystallogr., Sect. A: Found. Crystallogr.*, 2008, **64**, 112–122.
- 50 M. Save, M. Schappacher and A. Soum, *Macromol. Chem. Phys.*, 2002, **203**, 889–899.